Original article

Physiological basis and clinical significance of left ventricular suction studied using echo-dynamography

Motonao Tanaka (MD, FJCC)[a],*, Tsuguya Sakamoto (MD, FJCC)[b], Shigeo Sugawara (MD, FJCC)[a], Hiroyuki Nakajima (RMS)[a], Takeyoshi Kameyama (MD)[a], Haruna Tabuchi (MD)[a], Yoshiaki Katahira (MD)[a], Shigeo Ohtsuki (PhD)[c], Hiroshi Kanai (PhD)[d]

[a] Cardiovascular Center, Tohoku Welfare Pension Hospital, Fukumuro 1-12-1, Miyagino-ku, Sendai 983-0005, Japan
[b] Hanzomon Hospital, Kojimachi 1-14, Chiyoda-ku, Tokyo 102-0083, Japan
[c] Institute of Medical Ultrasound Technology, Yokoham 2-12-15, Sagamihara 229-1122, Japan
[d] Department of Electrical Engineering, Tohoku University, Aramaki-Aoba 6-6-05, Aoba-ku, Sendai 980-8579, Japan

Summary
Background: The existence as well as the exact genesis of left ventricular suction during rapid filling phase have been controversial. In the present study, we aimed at resolution of this problem using noninvasive and sophisticated ultrasonic methods. The clinical meaning was also documented.
Methods: Ten healthy male volunteers were examined by 2D echocardiography and echo-dynamography which enables us to obtain detailed instantaneous data of blood flow and wall motion simultaneously from the wide range of the left ventricle. The correlation of blood flow and wall motion was also studied.
Results: Rapid ventricular filling was divided into 2 phases which had different physiology. The early half (early rapid filling: ERF) showed the effect which was alike drawing a piston. This was proved by the shape of the velocity of inflow and the basal muscle contraction which actively assisted extension of the relaxed apical and central parts of the left ventricle, giving the negative pressure which causes the ventricular suction.

The later half (late rapid filling: LRF) showed the turning of the fundamental flow and the squeezed basal part just like the sphincter in addition to the expansion of the apical and central portions of the left ventricle, and all of these cooperatively augmented the suction effect.

* Corresponding author. Tel.: +81 022 719 5161; fax: +81 22 719 5166.
E-mail address: m.tanaka@jata-miyagi.org (M. Tanaka).

Conclusion: Ventricular suction does exist to help ventricular filling. Simultaneous appearance of the contraction in the basal part and the relaxation or extension in the apical part during the post-ejection transitional period was made to occur the suction in the LV. And it can be said that the suction appeared in the late stage of systole as the one of the serial systolic phenomena.

Introduction

Katz [1] speculated that ventricular suction during diastole might exist, and later on, Wiggers [2] mentioned an aspiration force might be generated whenever the elastic stress during contraction was released. Thereafter, the concept of diastolic suction has been disputed by Brecher [3] and others.

However, the previous studies dealt with only an excised and isolated heart preparation [4,5] or, at most, anesthetized animals [6—9]. Although human studies using a catheter-tip manometer [10—12] were able to measure pressure difference in the ventricle, the distinctive features, genesis, and physiological significance of the diastolic suction have been controversial. This was because these studies did not clarify the data concerning the pressure difference or transmitral flow velocity. This was also true as to the one-dimensional information of the ultrasonic Doppler method.

We attempted to clarify many facets of left ventricular suction in terms of blood flow structure and flow dynamics, regional wall dynamics, as well as their correlation using echo-dynamography [13,14] as previously reported.

Subjects and methods

Subjects

Ten healthy male volunteers aged 30—50 years who provided informed consent were the subjects.

Methods

The details were described partly in the previous articles [13—24].

Analysis of the blood flow structure in the left ventricle (LV) [13—18,23]
(1) Acquisition of flow velocity information

Special designed ultrasonic equipment (Alola Co., model 6500, Tokyo, Japan,) was used, and the recordings were made in the supine or lateral decubitus position. The scanning plane of the two-dimensional (2D) echocardiogram included 3 points, i.e. center of both the aortic and mitral orifices, and the ventricular apex. This plane had the advantage to analyze the blood flow field in the LV as previously mentioned [25]. 2D Doppler velocity was measured by apical approach and transferred to a personal computer. The data was processed off-line using the soft-ware of echo-dynamography [14—16,19,23,24]. Furthermore, phonocardiogram using a crystal acceleration microphone placed around the cardiac apex was recorded simultaneously with echocardiogrm and electrocardiogram.

(2) Analysis by using the 2D flow velocity vector distribution

As described previously [23—25], the Doppler velocity vector was obtained at many points, and the two dimensional distribution was displayed on the same scanning plane together with color Doppler signal and 2D echocardiogram (Fig. 1(1) and (2)).

(3) Analysis by the spread of main flow axis line

The meaning of the ridge line in the magnitude distribution of the flow vector was described previously [26]. The ridge line represents a main flow axis, and centralization of the power produced by the motion of the local ventricular wall and the transmission of the blood were shown. The wall function was evaluated by the changes of the pattern during the cardiac cycle [18,19,27] (Fig. 1(3) and (4)).

(4) Analysis by using the velocity profile along the main flow axis line

Displaying the flow velocity vector distribution, the magnitude distribution along the flow axis line was obtained as a one-dimensional curvilinear graph. Then, the inclination of the graph indicates the one of the convective acceleration of flow, and the integration indicates the flow volume [25] (Fig. 2).

(5) Analysis by using the Doppler pressure distribution on the scanning plane [14,18—20]

To deduce the influence of the dynamic pressure change to the distribution of flow velocity data, the Navier—Stokes' equation of motion was applied for the processing of the data [19]. This ''*Doppler pressure*'' was displayed by color on the 2D echocardiogram. The reference point was set at the area beneath the fibrous trigon (Fig. 3).

Analysis of the regional LV wall dynamics
(1) *Macroscopic* analysis using 2D echocardiogram

High speed sector scan of 66 frames/s was used to measure the thickness of the interventricular septum (IVS) and the posterior wall (PW) during cardiac cycle. The LV internal diameter at the apical (A), central (C) and basal (B) parts, as well as the diameter (MRD) and displacement (MRM) of the mitral ring were also measured. The images of successive 24 echocardiograms were used every 30 ms. The LV movement during one cardiac cycle was precisely analyzed as shown in Fig. 4.

(2) Analysis using free angle M-mode method

Using the memory of 2D echocardiogram of several cycles, M-mode echocardiograms were depicted to obtain the motion of the tissue of the oriented directions, so as to measure accurately various tissue movements simultaneously (named as free angle M-mode: FAM-mode). This method also enabled us to
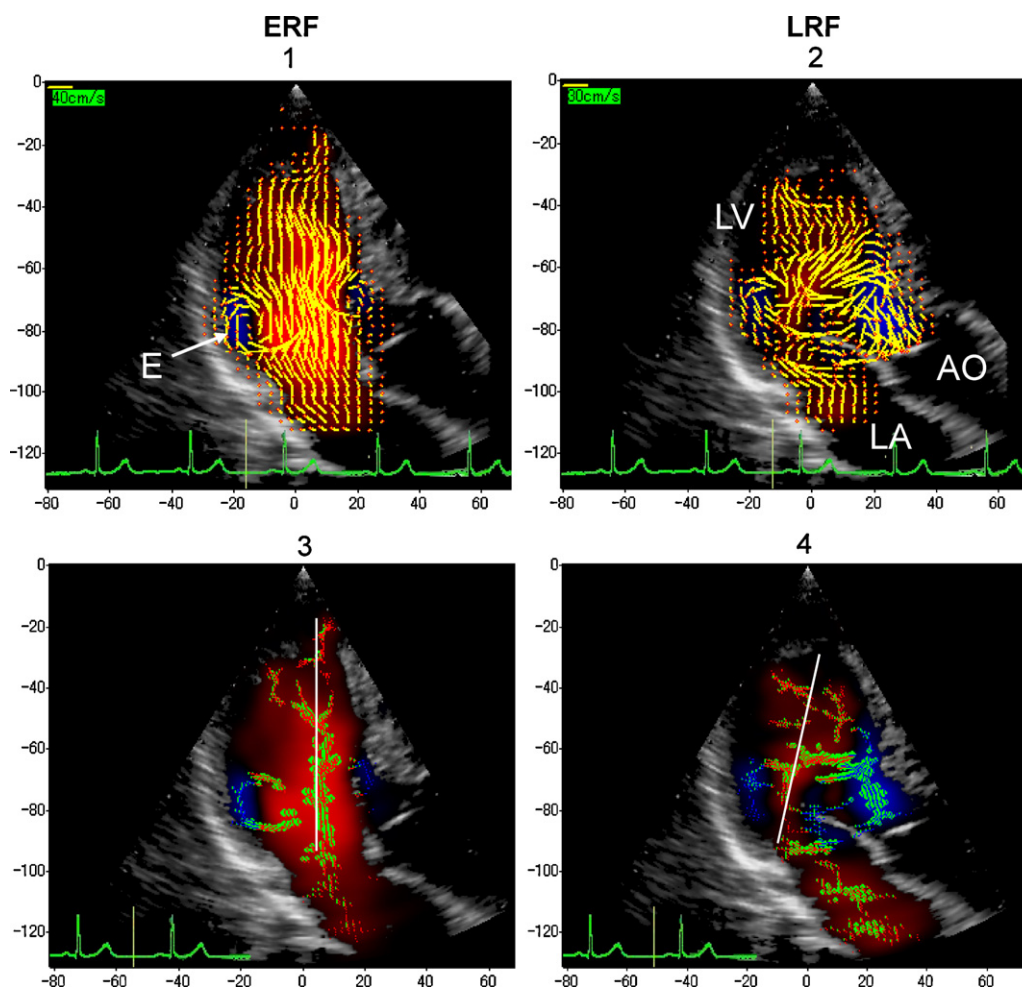
Figure 1 Upper images 1 and 2: Two-dimensional mapping of the flow velocity vector during rapid filling phase in the longitudinal section plane of the left ventricle in a normal case. The cardiac phase recorded the vector mapping is shown by the yellow line on the ECG. A reference size of the vector is shown by a yellow bar at the upper left corner of the mapping. A white arrow (E) shows the toroidal eddy flow. Bottom images 3 and 4: Two-dimensional distribution of the main flow axis line of the inflow into the ventricle in ERF (3) and LRF (4) shown by the overlapped display with the color flow imaging. White lines show the line for obtaining the flow velocity distribution along the main flow axis line shown in Fig. 2. ERF, early stage of the rapid filling; LRF, late stage of the rapid filling; AO, aorta; LA, left atrium; LV, left ventricle.

confirm the relationship between the minimal mitral valve ring and the maximal valve opening (Fig. 5).

(3) *Microscopic* analysis using strain rate (SR) distribution measured by the phase difference tracking method (PDT)

By switching beam direction at every 5° intervals (sparse scan), about 30° within the 90° sector angle was scanned at the speed of 630 frame/s. The moving velocity of the pulsating myocardium was measured, the thickness change in each direction was obtained at every thickness interval of 0.82 mm by the PDT [21]. This was based on the assumption that the sound speed in the myocardium is 1600 m/s [28]. The SR thus obtained was overlapped on the M-mode and 2D images, respectively, as a color corded information [22] (Figs. 6 and 7).

(4) Measurement of LV internal diameter

Using PDT, the change in the LV internal diameter was exactly measured by looking the moving speed of the 2 target points set on the endocardium of the PW and IVS. This was displayed by the curvilinear graph together with electrocardiogram and phonocardiogram (Fig. 7).

Results

Blood flow structure in the LV demonstrated by flow velocity vector

During rapid filling, two types of flow velocity vector distribution widely spread in the longitudinal sector plane were seen from the mitral valve (MV) orifice to the apex as follows (Fig. 1):
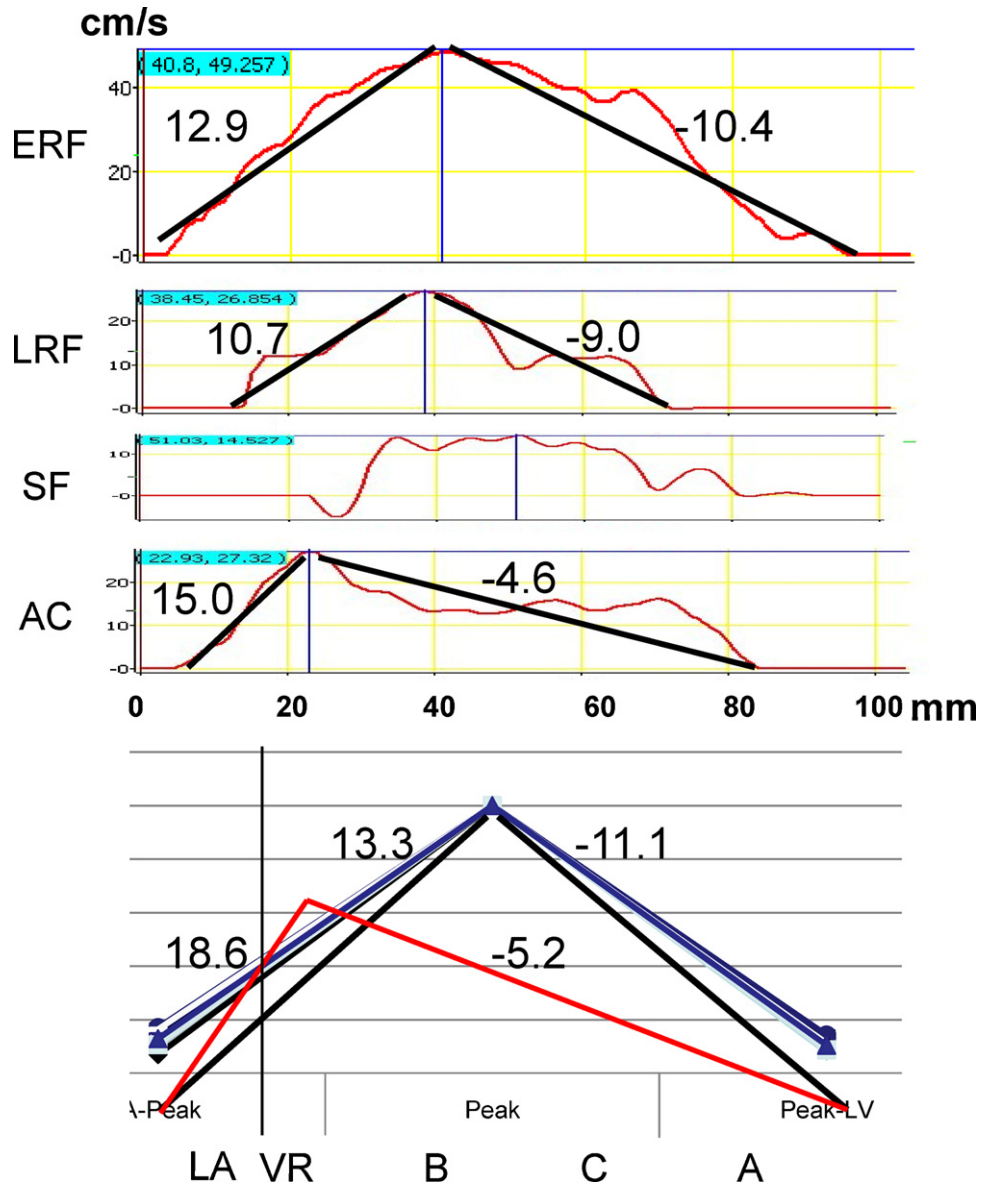
Figure 2   Upper four graphs: Velocity distribution (red zigzag curvilinear lines) and velocity gradient (black lines) along the main flow axis line (shown in Fig. 1(3) and (4)) of the inflow into the left ventricle during the ERF, LRF, SF, and AC phases. Bottom graph: Velocity gradient on the main flow axis line in the ERF obtained from 10 normal cases. The black line indicates the mean value of the gradient. The inclination of the gradient is almost the same in all normal cases. The red line shows the mean value of that in the AC. In AC, the inclination of the gradient was different in atrial side from that in apical side. ERF, early stage of the rapid filling; LRF, late stage of the rapid filling; SF, slow filling; AC, atrial contraction; LA, left atrium; VR, mitral valve ring position; B, basal part; C, central part; A, apical part; Abscissa shows velocity in mm/sec, and Ordinate, distance in mm.

(1) During ERF

The flow velocity vector directed rather straight to the apex with a minor zigzag pattern. Though the circularly arranged vectors (E) due to the toroid-like eddy probably resulting from the flow separation was observed behind the MV tips, no reversal or reflected flow was observed at the inner surface of the LV (Fig. 1, ERF).

The main flow axis line was nearly straight from the center of the MV orifice to the apex, and thereafter 3 branches of the axis line were observed behind the papillary muscle area (Figs. 1—3). The velocity profile along the main flow axis line showed ''ups and downs'' of shape (Fig. 2-ERF; black lines), and the summit was near the center of the basal part at the maximal part of the LV short-axis diameter. The velocity gradients in the MV orifice side (acceleration) and apical side (deceleration) were ca. 12.9 and ca. −10.4, respectively (black lines).

The averaged velocity gradients from 10 subjects were 13.3 (acceleration) and −11.1 (deceleration), respectively (black lines in Fig. 2 bottom).
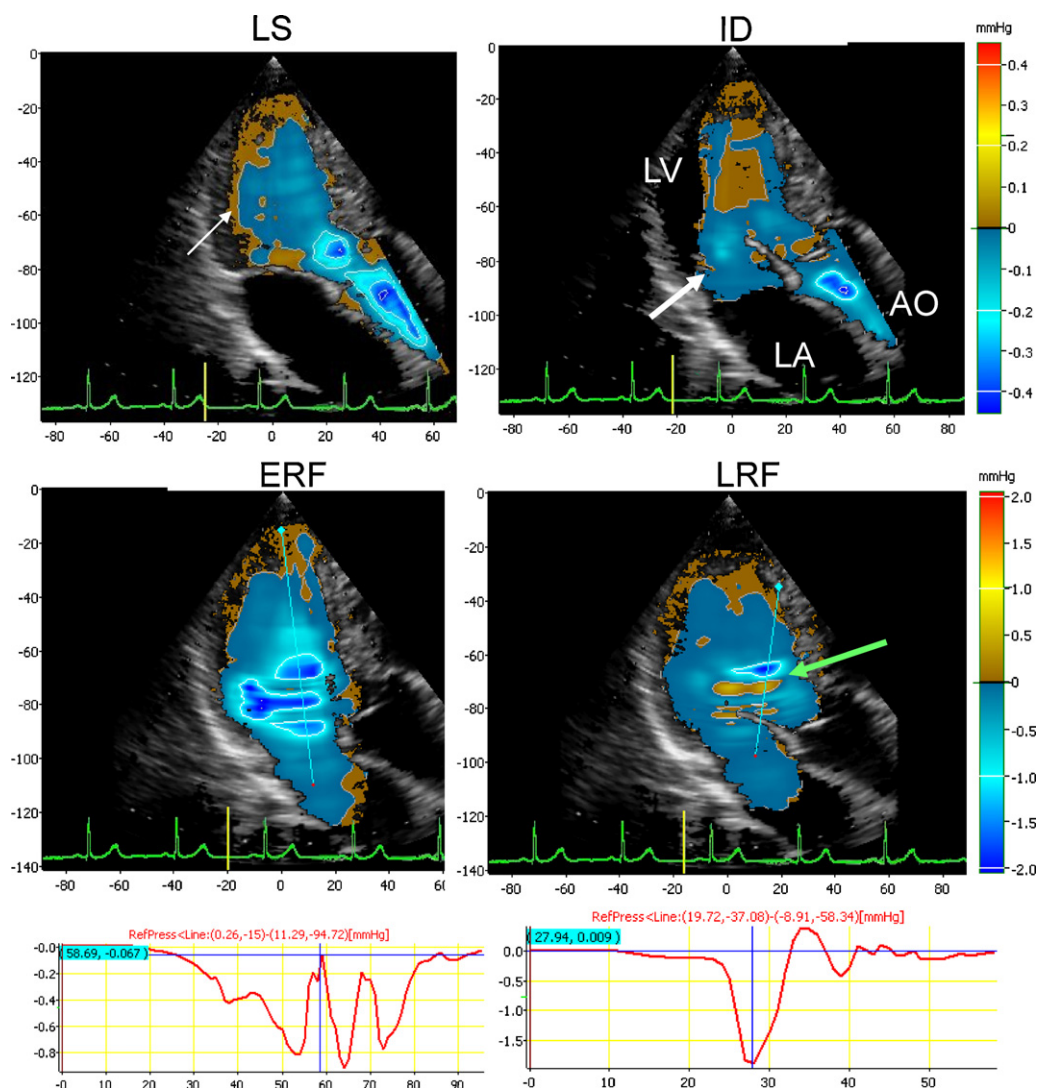
Figure 3 Two dimensional distribution of the Doppler pressure (dynamic pressure) in the left ventricle in the four cardiac phases. Cold colored area shows the negative pressure and warm colored area, the positive pressure. Pressure level is indicated in the color bar in the right column. Narrow white arrow, the negative pressure appeared in the area just behind the posterior wall during the initial stage of the sucking action even during the systolic phase. Wide white arrow, the increasing negative pressure at the beginning of the upward movement of the mitral valve ring. Green arrow, oscillation of the pressure wave indicating the origin of the third heart sound. Bottom graphs are one dimensional display of the pressure distribution along the blue lines on the 2D images. Oscillating pressure pattern are clearly observed (green arrow). LS, late systolic phase; ID, isovolumetric dilatation phase; ERF, early stage of rapid filling; LRF, late stage of rapid filling; AO, aorta; LA, left atrium; LV, left ventricle.

(2) During LRF

The distribution of the velocity vector of the inflow blood widely spread (Figs. 1—2 LRF). As to the toroid-like eddy and reversal or reflected flow at the apical area, the same was true as in ERF.

The main flow line was divided in 2 ways. The one was main and curved anteriorly at the center of the LV, and the other was divided into 3 branches directing to either the apical or anterior or posterior areas behind the papillary muscles (Figs. 1—4). The main flow further directed behind the anterior MV and collided with the reverse side of the leaflet, causing resonant oscillation of pressure wave. This was demonstrated as a pile of the cold and warm color strips (green arrow in Fig. 3; LRF). The velocity vector profile was also ''ups and downs'' shaped similar to that of ERF, and the summit was lower about 50% than that of ERF (Fig. 2: LRF). The velocity gradients were 10.7 in the acceleration side and −9.0 in the deceleration side, respectively. However, velocity gradient at the beginning and ending points was slightly greater than those of ERF.

2D Doppler pressure distribution

Even during late systolic phase (LS), negative pressure of about −0.04 mmHg was observed at the central and basal
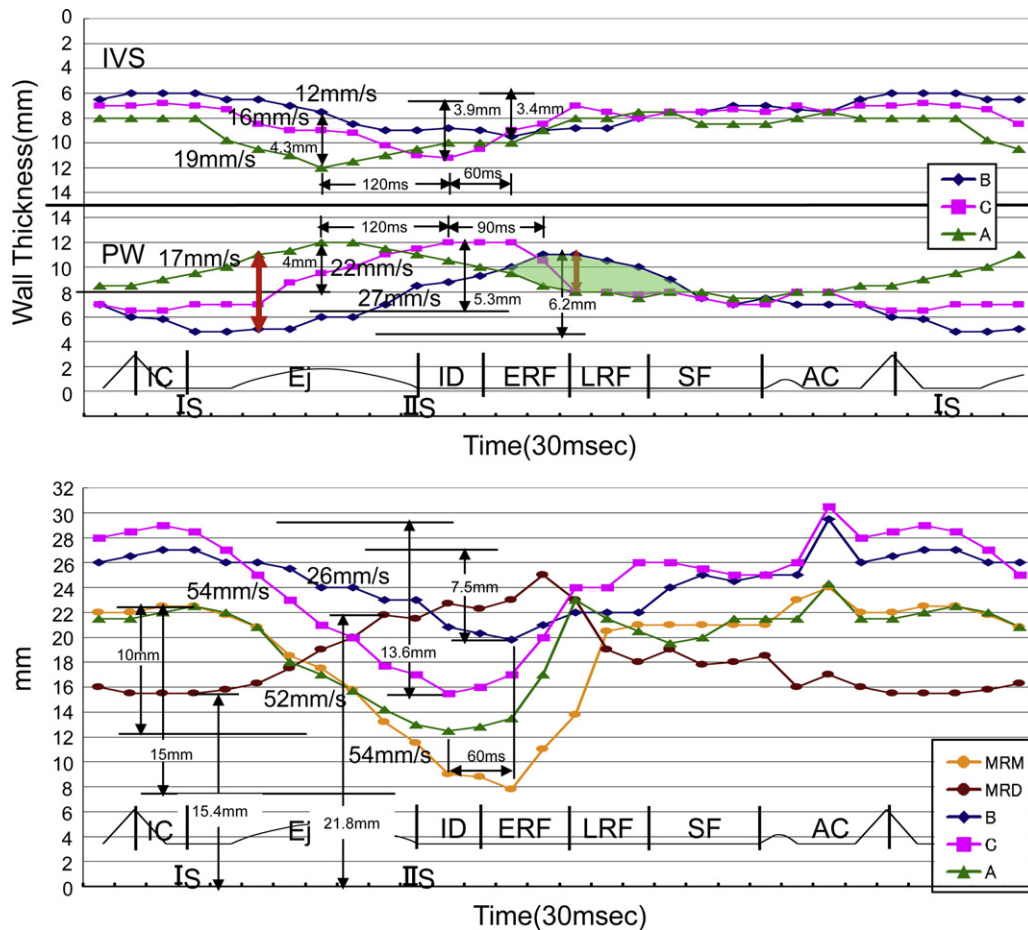
Figure 4 Top graph, Changes in thickness of the posterior wall (PW) and the inter-ventricular septum (IVS) measured at 3 parts of basal (B, blue line), central (C, red line), and apical part (A, green line) of the left ventricle during one cardiac cycle. Bottom graph, Changes in the internal diameter of the left ventricle at the 3 parts of basal (B), central (C) and apical (A), and of the mitral ring diameter (MRD, brown), and changes in distance of the upward displacement of the posterior part of mitral ring during one cardiac cycle (MRM, yellow). The measurement was performed from the two-dimensional echo-cardiograms obtained in the longitudinal direction of a normal left ventricle. The number shows a speed and distance of the change. IVS, Inter-ventricular septum; PW, posterior wall; Is, 1st heart sound; IIs, 2nd heart sound; IC, isovolumetric contraction; Ej, ejection; ID, isovolumetric dilatation; SF, slow filling; AC, atrial contraction; ERF, early stage of rapid filling; LRF, late stage of rapid filling; Green shaded area; the phase in which the contracting and extending parts coexist in the ventricular wall.

areas near the inner surface of the PW (thin white arrow in Fig. 3: LS).

During isovolumetric dilatation (isometric relaxation: Fig. 3: ID), negative pressure areas appeared near the inner surface of the LV wall and beneath the valve rings (thick white arrow). The measurement value was −0.07 and −0.13 mmHg beneath the aortic and mitral valve, respectively, and −0.03 mmHg at the apical area near the PW. Therefore, the negativity of the basal area was 2−4 times greater than those at the other areas.

During ERF (Fig. 3-ERF), such a widely spread negativity and a resonance of the negative pressure were seen from the MV orifice to the apex along the LV long axis, and the lowest was −1.2 mmHg in the central and basal area. The pressure gradient along the inflow axis line was about 0.46 in the orifice side and was about 0.32 in the apical side.

During LRF (Fig. 3-LRF), positive pressure area spread over the apical area, while negative one appeared widely in the central and basal areas along the short axis. At the same time, the minimal pressure (ca. −1.8 mmHg) was in the center of the outflow area near the IVS, and the pile of the positive and negative pressure areas was seen behind the anterior mitral valve, resulting in the pressure oscillation (green arrow).

LV wall dynamics *macroscopically* observed by 2D echocardiography and FAM

Thickness of the IVS and the PW at the apical area decreased during rapid filling phase (line A: green in Fig. 4), while the internal LV diameter increased rapidly in ERF and then slowly in LRF (Fig. 4 top).

At the mid-ventricular level (central area: line C: red), the PW thickness increased in the mid-ERP and decreased rapidly in LRF, while the IVS thickness decreased. The LV
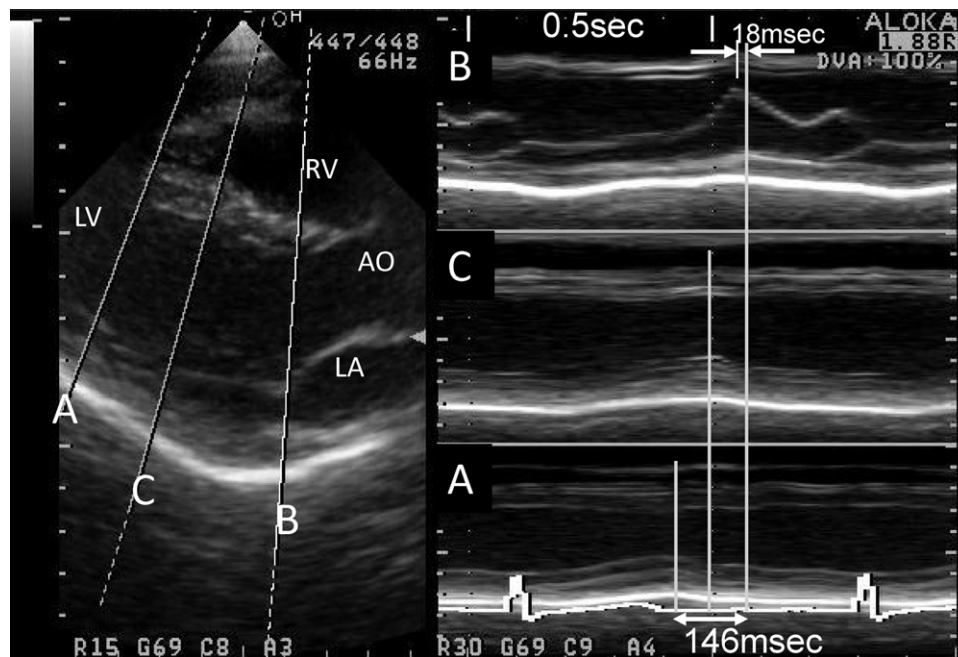
Figure 5 The free angle M-mode display of the left ventricular wall and mitral valve. M-mode display of the ventricular wall at basal (B), central (C) and Apical (A) parts for measuring the time when the maximum inward displacement of the wall appeared. AO, aorta; LA, left atrium; LV, left ventricle; RV, right ventricle.

internal diameter increased rapidly in ERF and then slowly in LRF.

At the basal area (line B: blue), the PW thickness increased until mid-LRF, while the LV diameter decreased until the end of ERF and then gradually increased in LRF. No apparent changes were seen in the IVS thickness.

The timing of the maximum thickness of the PW was delayed in B compared to A by about 210msec, and that of the minimal internal diameter of the LV was similarly delayed in B. This indicated that contraction and extension were transmitted dispersively, resulting in the peristalsis of the LV wall [25].

After the maximal MRD (brown line) reached the end of ERF, it decreased rapidly in LRF. The FAM-mode image showed time lag of about 18msec in the minimal size of the MRD compared to the maximal MV opening (Fig. 5), while the posterior part of the mitral ring (MR) moved toward the left atrium (LA) (Fig. 4 bottom: MRM: yellow line). This indicated that LV predominantly dilated longitudinally at the basal part of the LV.

During rapid filling phase, as indicated by the shaded area in Fig. 4 top, the muscle in basal area (B) was contracting, whereas the muscle in apical area (A) was in the reversed behavior, i.e. the contracting and extending state occurred at the same time process. Also, the maximal thickness of the basal part of the PW coincided in time with the minimal thickness of the apical and central parts of the PW, and further the boundary between ERF and LRF nearly coincided in time with the summit of E of Doppler velocity curve. These facts indicated the basal muscle contraction tempted in the relaxed apical and central muscles to extend.

Microscopic LV wall dynamics analyzed by strain rate (SR) distribution

In Fig. 6, positive SR (+) (cold color; blue) indicates contraction, and negative SR (−) (warm color), either relaxing (red) or extending (yellow) state.

(1) During ERF
   (a) PW (Fig. 6)
       The apical endocardial side was in the relaxing state (SR: nearly 0), and the epicardial side was in extending state (SR = ca. −4.0) (Fig. 6(3)). The central part showed a sandwitched pattern (Fig. 6(2)), i.e. contracting and extending states were piled. The contraction was mainly in endcardial side and the extension was mainly in epicardial side as well as in the mid-layer between these two sides. Furthermore, the string-like narrow contracting area was seen near the epicardial side (vertical white arrow C). The basal part (Fig. 6(1)) showed a large contraction in the endocardial side during the first half of ERF, whereas it changed to large extension in the second half of ERF. Extension was also seen in epicardial side and again string-like contraction was observed.
   (b) Interventricular septum (IVS)
       Contraction and extension were mixed in the apical and central areas, and extension was seen in the basal area. The tension state persisted in the apical and central areas, whereas extension persisted in the basal area.
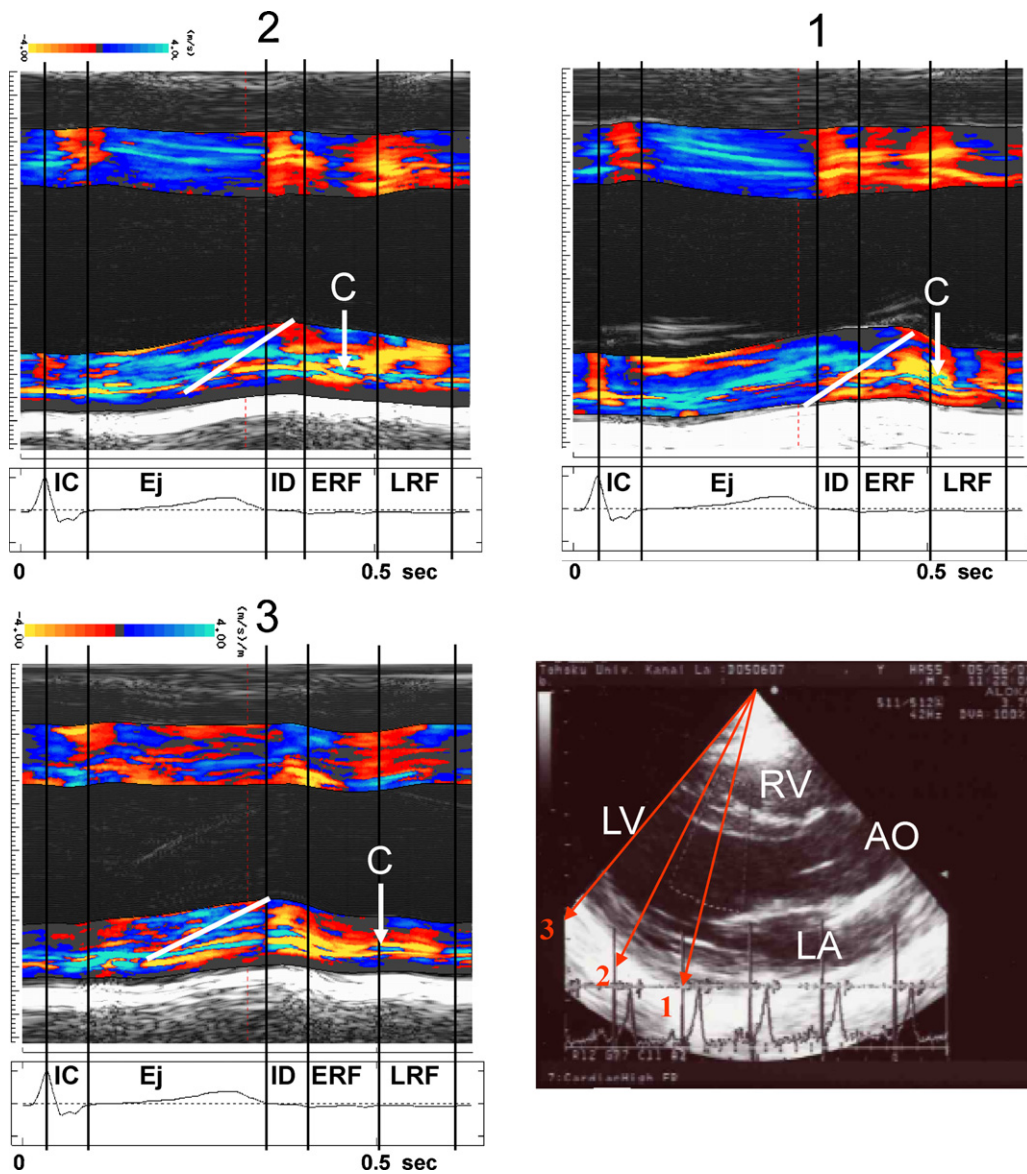
Figure 6 M-mode images of the strain rate (SR) distribution in the time sequential change in the intra-ventricular septum (IVS) and posterior wall (PW) measured by using the sparse scan and the phase difference tracking method on the longitudinal section plane of the left ventricle (LV). The SR was obtained in the beam direction of 1—3 shown on the two dimensional echo-cardiogram in the right below. The cold color area shows an increment of the SR (contraction) and the warm color area shows a decrement of the SR (extension) as demonstrated in the color bar. IC, isovolumetric contraction; Ej, ejection; ID, isovolumetric dilatation; ERF, early stage of rapid filling; LRF, late stage of rapid filling; White arrow C, contracting muscle layer; Oblique white line, spreading process of the extending area in the LV wall; AO, aorta; LA, left atrium; LV, left ventricle; RV, right ventricle.

(2) During LRP

  (a) PW

At the apical area, there was a large extending part in the epicardial side, whereas a relaxing part was present in the endocardial side. At the central area, a large extension was in the mid-layer, but contraction was in the endocardial side, and a string-like narrow contracting area was near the epicardial side (Fig. 6(2), thick white symbol C) which continued from that of ERF. At the basal area, a large area of extension continued from that of ERF was shown in the mid-layer and epicardial side. Contracting area was seen in the mid-layer and endocardial side. During the second half, extension was seen through endocardial to epicardial side. Near the epicardial side, string-like narrow contracting area was again observed (Fig. 6(1), thick white symbol C).

  (b) IVS

A mixture of contracting and extending areas was seen in the area from the apical to the basal part. This indicated that the IVS was in tension state in LRF.

(3) SR distribution
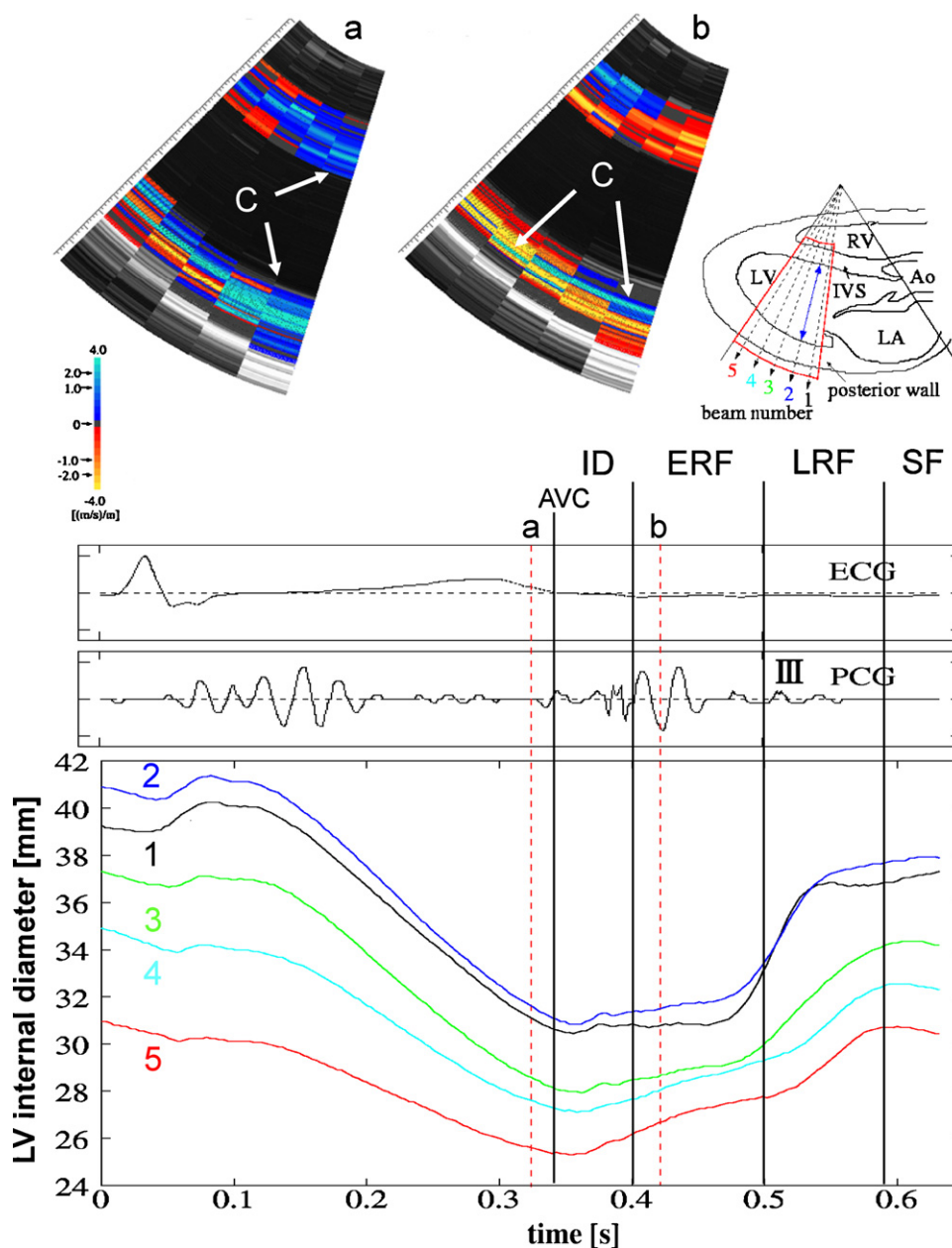
Figure 7 Upper 2 images show the two dimensional SR distribution in the time point of (a) and (b) on the ECG and PCG at the lower graph. The contracting area (C) in figure b observed at the part near the epicardium was supposed to be the oblique muscle layer of the ventricular musculature, and (C) in figure a at the middle and endocardial parts near the valve ring at the basal part supposed to be circumferential layer. Lower graph shows changes in the internal diameter of the left ventricle during systole through rapid filling phase measured by the phase tracking method in the 5 beam directions (1—5) shown in the right upper side picture. Beams 1 and 2, basal part; Beams 3 and 4, central part; Beam 5, apical part; AO, aorta; LA, left atrium; LV, left ventricle; RV, right ventricle; III, third heart sound; ID, isovolumetric dilatation; ERF, early stage of rapid filling; LRF, late stage of rapid filling; SF, slow filling; AVC, aortic valve closure; ECG, electrocardiogram; PCG, phonocardiogram.

As described above, SR distribution demonstrated that contraction and extension of the myocardium occurred simultaneously in the LV wall. Namely, a contracting area at the basal part of the LV near the valve ring and remarkable extension in the short axis direction at the central and apical areas in addition to dilatation of the apex were simultaneously observed.

LV expansion in short axis direction (Fig. 7)

During ERF, LV diameter increased slowly at the apical area (red line) and center area (green line), whereas the change was minimal at the basal part (black line). This indicated that LV volume during ERF increased predominantly along the longitudinal axis.

On the other hand, LV diameter during LRF slowly increased at the apical area (red line), slightly faster at the central part (green line), and fastest at the basal part (black line). These results indicated that LV volume during LRF increased predominantly along the shot axis.

The third heart sound (III)

As shown in Fig. 7, the III was inscribed in the PCG coincided in time with the rapid expansion along the short axis. Superimposition of Figs. 3 and 7 confirmed that the III occurred coinciding with the pressure oscillation within the LV (Fig. 3, green arrow).

Discussion

The left ventricular relaxation process in diastolic filling was first described by Katz [1], and Wiggers [2] discussed the role of diastolic suction.

Experimental studies were done by Brecher [3], but the pressure variation during rapid filling is so small that it is unable to explain a large amount of ventricular blood inflow during a very short time, particularly in animals with very rapid heart rate and extremely short diastolic filling time [4,5]. Furthermore, many physiological conditions including even the atmospheric pressure may change, so that the results of animal experiments may not be worthy of evaluation. The similar results using intracardiac pressure evaluation [6,7,9,12] or ultrasonic Doppler method [9—11] were not reliable, because spatial structure of intraventricular blood flow, pressure distribution within the LV, local ventricular wall dynamics and their correlation were all difficult to estimate by these methods. The present study suggested that left ventricular suction involved a complicated mechanism, and that only noninvasive method such as our echo-dynamography might resolve the above-mentioned difficulties.

We have already pointed out that the ventricular suction started at the late stage of the systole [25], and the distinctive feature of suction appeared in the ERF phase. As Courtois [7] reported using pressure measurement method that this filling consisted of 2 phases, and further verified the boundary of these two phases coincided in time with the E wave of the Doppler velocity curve. We proved further that these 2 phases contributed differently to the ventricular suction during rapid filling phase.

As to the ERF phase, we disclosed that the inflow occurred with less resistance and less inertia to draw the blood into the LV, because of the correspondence of the direction of ventricular dilatation and inflow. This is such that a piston effect along the long axis without the commitment of short axis dilatation.

On the other hand, ventricular filling during LRF phase was quite different in terms of division of flow direction. Such a division was caused mainly by the active dilatation of the central and basal areas of the LV along the short axis, so as to increase the LV volume and was also helpful to pour the inflow blood into the outflow tract which was just like a dead space during ERF.

The previously advocated theory of ventricular suction was based on the assumption of myocardial elastic recoil during diastole [6,9,12,29—31], which was caused by the release of potential energy accumulated within the muscle during systole [32—34]. This assumption has several ambiguous points. For example, they did not consider the discordant movements of the local LV wall, instantaneous geometric changes of the LV and intraventricular flow structure within the LV.

Certainly, LV suction may require active negative pressure during diastole and the present study proved the widely spread negativity which was spatially changing in time with the wall dynamics. All facts considered, the correlation between the wall and flow dynamics is schematically summarized as shown in Fig. 8.

Sengupta et al. [35] stated that the mechanical shortening of the LV propagated from apex to base, as did the electrical transmission.

However, our study disclosed that this delay was due to the peristalsis [25], and at the end of systole, muscular contraction propagated to the basal part near the mitral valve ring, whereas the apical and central parts of the PW were in the completely relaxed and extended state (as demonstrated by green shadow in Fig. 4). Important facts were that, during ERF, these relaxing (SR = 0) and extending (SR = −) parts were pulled rapidly parallel to the long axis direction along with the upward movement of the mitral valve ring. There was no simultaneous extension along the short axis. On the other hand, LV extension at the central and apical parts appeared along the short axis direction during LRF.

We postulated that these wall dynamics might have a relationship to the anatomy of the ventricular muscles. As well known, myocardium has 3 muscle layers, including middle circular muscle which is thick, and internal and external oblique muscles which are running along each other in the opposite direction [36—40]. The upper margin of the muscle fuses tightly with the fibrous aortic and mitral valve rings which are also tightly fastened to each other at the fibrous trigon, and thereby the mitral ring has a hinge-like mobility.

When this anatomy was compared with our SR data, it is not difficult to speculate that symbol C in Figs. 6 and 7b are both oblique muscle group, while symbol C in Fig. 7a is that of circular muscle. This means whenever the basal muscle layer is in the contracting state (SR+), the central and apical muscles are in either relaxing (SR 0) or extending (SR−) state. Namely, the contracting and extending areas co-exist separately in the LV wall.

This phenomenon is illustrated in the bottom of Fig. 8, and this makes it easy to understand the underlying mechanism of ventricular suction.

With the strong contraction of the circular muscle (Cir) (thick and blue arrow), the posterior part of the mitral valve ring is vigorously pulled toward the interventricular septum of high tension and is further pulled up toward the left atrium (vertical blue arrow) by the hinge-like motion of the fibrous trigon as a fulcrum (black arrow). And then, the narrowed mitral valve orifice causes shortening of the antero-posterior diameter of the valve (thin horizontal blue arrow), and the already relaxing and extending central and apical parts of the PW remain almost unchanged. Thus, this is the reason of LV volume increase due to the suction during ERF.
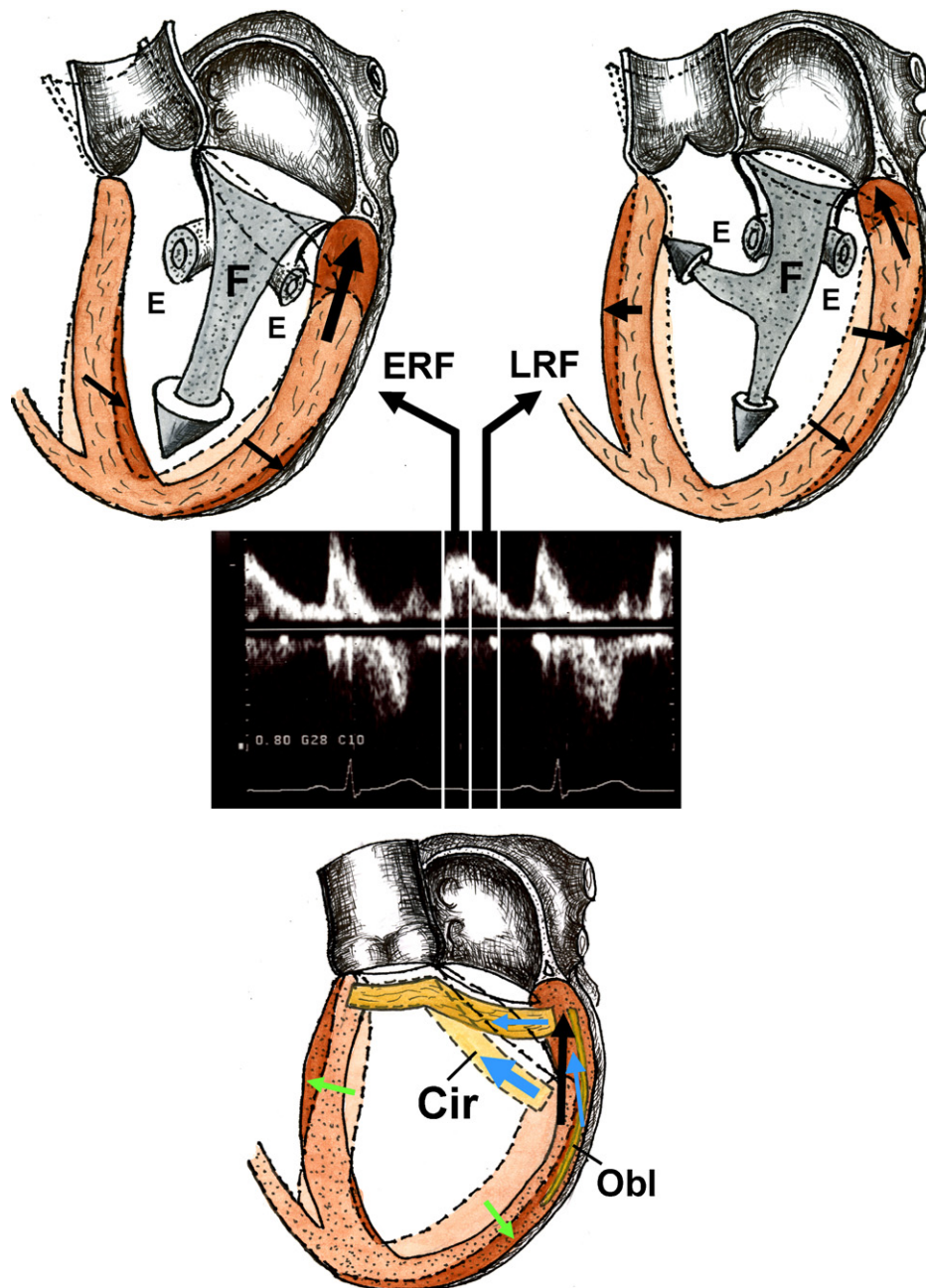
Figure 8 Schematic representation of the correlation among the flow structure, wall dynamics and Doppler flow velocity during the rapid filling phase (upper two images), and of the correlation between the muscle orientation and the contraction process in the basal part of the ventricle (lower image). E, toroidal eddy produced by the separation of flow at the edge of the mitral valve leaflets; Gray large arrows F, main inflow; Black arrows, direction and magnitude of the extension and contraction of the moving ventricular muscle; Green arrows, extending direction; Blue arrows, direction of the muscle contraction; FRF, early stage of rapid filling; LRF, late stage of the rapid filling; Cir, circumferential muscle layer; Obl, oblique muscle layer.

The mechanism of ventricular suction during LRF is as follows: when both inner and outer oblique muscles contract efficiently (thin vertical blue arrow positioned laterally in the figure), the basal part of the PW further displaces upward and posteriorly. Then, the antero-posterior diameter of the mitral valve ring diminishes and the valve ring becomes oval-shaped. This narrowing of the valve ring is caused by the sphincter action of the circular muscle.

Furthermore, the central and a part of the basal areas are further extended in the short axis direction (green arrows), resulting in the suction during LRF.

In fact, ventricular suction described herein is thought to be one step of a series of ventricular systolic action. The energy required for such suction might be supplied by the contraction of the basal myocardium. Many previous clinical reports [10,12,29] suggested that myocardial contractility

was improved whenever ventricular suction was restored. This was thought to be consistent with the previous experimental results [7–9,11].

Ventricular suction had some connections to the mechanism of heart sound production. In the present study, the third heart sound is thought to be generated by the vibration of either mitral valve or ventricular muscle coincident with the sudden decrease or halt of the rapid ventricular filling [41–43]. Courtois [7] suggested that the place of production was the apical ventricular wall, because pressure reversal of a high degree was observed around the apex. However, the present study disclosed that actively extending apical area causes inflow without resistance, so that the vibration of the apex is unbelievable. Actually, the third heart sound was recorded consistent in time with LRF. During this period, blood inflow passed the outflow and reached the reverse side of the mitral valve and collided with this valve. The pressure was reflected and transmitted to the IVS, resulting in the oscillation of blood of back-and-forth between the valve and the IVS. Thus, alternate positive and negative pressure areas were seen in the outflow area (green arrow in Fig. 3-LRF). This indicated that the occurrence of low frequency vibration might be the resonance of the pressure wave in accord with the vibration theory of the cardiohemic system [42,44].

Conclusion

Using echo-dynamography newly developed, physiological and clinical features of left ventricular suction during rapid filling phase were investigated.

The suction developed by inhaling inflow blood by two ways. One was the ERF, during which the apical part was expanding along the long axis of the left ventricle, causing the suction by the piston effect. The second was the LRF, which was separated from ERF by the summit of the E wave of Doppler velocity curve, and during which blood supply of inflow was due to the expansion in the short axis of the basal part toward the outflow, causing additional volume increase in the left ventricle.

In these manners, both contraction and extension coexist within the left ventricle during rapid filling phase and the effectiveness of suction was thus enhanced.

For these mechanisms, systolic contraction of the basal part during ERF phase, which was followed to the late stage of ventricular contraction, played an important role. The energy of suction was supplied by this basal muscle contraction.

The possible relationship of the mechanism of suction and the structure of the ventricular muscle layer was discussed in detail.

Clinically, the mechanism of generation of the third heart sound was thought to be derived from the resonance of pressure between the anterior mitral valve and the intervenricular septum.

References

[1] Katz L. N. The role played by the ventricular relaxation process in filling the ventricle. Am J Physiol 1930;95:542–53.

[2] Wiggers CJ. Cardiac mechanisms that limit operation of ventricular suction. Science 1957;126:1237.

[3] Brecher GA. Critical review of recent work on ventricular diastolic suction. Circ Res 1958;6:554–66.

[4] Brecher GA, Kissen AT. Ventricular diastolic suction at normal arterial pressures. Circ Res 1958;6:100–6.

[5] Brecher GA. Experimental evidence of ventricular diastolic suction. Circ Res 1956;4:513–8.

[6] Hori M, Yellin EL, Sonnenblick EH. Left ventricular diastolic suction as a mechanism of ventricular filling. Jpn Circ J 1982;46:124–6.

[7] Courtois M, Kovacs Jr SJ, Ludbrook PA. Transmitral pressure-flow velocity relation. Impact of regional pressure gradients in the left ventricle during diastole. Circulation 1988;78:661–71.

[8] Courtois M, Kovacs SJ, Ludbrook PA. Physiological early diastolic intraventricular pressure gradient is lost during acute myocardial ischemia. Circulation 1990;81:1688–96.

[9] Firstenberg MS, Greenberg NG, Garcia MJ, Thomas JD. Relationship between ventricular contractility and early diastolic intraventricular pressure gradient: a diastolic link to systolic function. J A S E 2008;21:501–6.

[10] Steine K, Stugaard M, Smiseth OA. Mechanisms of retarded apical filling in acute ischemic left ventricular failure. Circulation 1999;99:2048–54.

[11] Yotti R, Bermejo J, Antoranz JC, Desco MM, Cortina C, Rojo-Alvarez JL, Allue C, Martin L, Moreno M, Serrano JA, Munoz R, Garcia-Fernandz A. A noninvasive method for assessing impaired diastolic suction in patient with dilated cardiomyopathy. Circulation 2005;112:2921–9.

[12] Udelson JE, Bacharach SL, Cannon 3rd RO, Bonow RO. Minimum left ventricular pressure during beta-adrenergic stimulation in human subjects. Evidence for elastic recoil and diastolic ''suction'' in the normal heart. Circulation 1990;82:1174–82.

[13] Tanaka M. Usefulness of ultrasonic imaging in medical field. In: Shimizu H, Chubachi N, Kushibiki J, editors. Acoustical imaging, vol. 17. New York: Plenum Press; 1989. p. 453–66.

[14] Tanaka M. Historical perspective of the development of echo-cardiography and medical ultrasound. In: Schneider SC, Levy M, McAvoy BR, editors. Proceed of the IEEE Ultrasonics Symp, vol. 2. NewYork: IEEE Inc; 1998. p. 1517–24. Available: http://www.ieee-uffc.orig/ultrasonics/teaching/us0000.pdf [February 2002].

[15] Tanaka M, Yamamoto A, Endo N, Takahashi K, Ohtsuki S. Evaluation of the behavior of blood flow in heart chambers by means of stream line distribution method. In: The visualization society of Japan, edit. Atlas of visualization. Oxford: Pergamon Press; 1993. p. 205–19.

[16] Ohtsuki S, Tanaka M, Okujima M. A method of flow vector mapping deduced Doppler data on sector scanned plane. In: Shimizu H, Chubachi N, Kushibiki J, editors. Acoustical imaging, vol. 17. NewYork: Plenum Press; 1989. p. 467–72.

[17] Tanaka M, Nitta S, Yamamoto A, Takahashi K, Saijo Y, Ohtsuki S. Development and application of non-invasive method for the evaluation of cardiac function, quantifying intracardiac blood flow. Asian Med J 1994;37(5):283–6.

[18] Tanaka M, Nitta S, Yamamoto A, Sato N, Takahashi K, Saijo Y, Ohtsuki S, Ohomote R, Ohba K, Ohno H. Development and application of non-invasive methods for the evaluation of cardiac function: Measuring cardiac function. Asian Med J 1994;37(7):397–400.

[19] Ohtsuki S, Tanaka M. Doppler pressure field deduced from the Doppler velocity field in an observation plane in a fluid. Ultrasound Med Biol 2003;29:1431–8.

[20] Tanaka M, Nitta S, Yamamoto A, Takahashi K, Saijo Y, Ohtsuki S. Development and application of non-invasive method for the evaluation of cardiac function: visualization of pressure changes in heart chambers. Asian Med J 1994;37(6):341–4.

[21] Kanai H, Hasegawa H, Chubachi N, Koiwa Y, Tanaka M. Non-invasive evaluation of local myocardial thickening and its color-coded imaging. IEEE Trans Ultrson Feroelect Freq Control 1997;44(4):752—68.

[22] Kanai H, hasegawa H, Chubachi N, Koiwa Y, Tanaka M. Non-invasive evaluation of spatial distribution of local instantaneous strain energy in heart wall. In: Lees S, Ferrari LA, editors. Acoustic imaging, vol. 23. New York: Plenum Press; 1997. p. 187—92.

[23] Ohtsuki S, Tanaka M. The flow velocity distribution from the Doppler information on a plane in three dimensional flow. J Visual 2006;9:69—82.

[24] Ohtsuki S, Tanaka M. Flow function for streamlines representative of the flow on a plane in three-dimensional flow. J Visual Soc Jpn 1998;18:136—40.

[25] Tanaka M, Sakamoto T, Sugawara S, Nakajima H, Katahira Y, Ohtsuki S, Kanai H. Blood flow structure and dynamics, and ejection mechanism in the left ventricle: analysis using echo-dynamography. J Cardiol 2008;52:86—101.

[26] Nakajima H, Tanaka M, Sugawara S, Katahira Y, Ohtsuki S. Clinical significance of the velocity distribution on the flow axis line for evaluating the left ventricular function. J Cardiol 2004;44(Suppl.):428 [abstract].

[27] Schoephoerster RT, Silva CL, Ray G. Evaluation of left ventricular function based on simulated systolic flow dynamics computed from regional wall motion. J Biomech 1994;27:125—36.

[28] Tanaka M, Dunn F. Acoustic properties of the fibrous tissue in myocardium and detectability of the fibrous tissue by the echo method. In: Dunn F, Tanaka M, Ohtsuki S, Saijo Y, editors. Ultrasonic tissue characterization. Tokyo: Springer-Verlag; 1996. p. 231—43.

[29] Nikolic S, Yellin EL, Tamura K, Vetter H, Tamura T, Meisner JS, Frater R. W. Passive properties of canine left ventricle: diastolic stiffness and restoring force. Circ Res 1988;62:1210—22.

[30] Nikolic S, Feneley M, Pajaro O, Rankin J, Yellin E. Origin of regional pressure gradients in the left ventricle during early diastole. Am J Physiol 1995;268:H550—7.

[31] Firstenberg MS, Smedira NG, Greenberg NL, PriorDL, McCarthy PM, Garcia MJ, Thomas JD. Relationships between early diastolic interventricular pressure gradients, an index of elastic recoil, and improvement in systolic and diastolic function. Circulation 2001;104. I-330-5.

[32] Rushmer RF. Functional anatomy and control of the heart. In: Rushmer RF, editor. Cardiovascular dynamics. 4th ed. Philadelphia: WB Sounders Co; 1976. p. 98.

[33] Ishide N, Takishima T. Cardiodynamics and its clinical application. 2nd ed. Tokyo: Bunkodo Co; 1992. p. 121—2.

[34] Braunwald E, Sonnenblick EH, Ross Jr J. Contraction of the normal heart. In: Braunwald E, editor. Heart disease. 2nd ed. Philadelphia: WB Sounders Co; 1984. p. 409—46.

[35] Sengupta PP, Khandheria BK, Korinek J, Wang J, Jahangir A, Seward JB, Belohlavek M. Apex-to-base dispersion in regional timing of left ventricular shortening and lengthening. JACC 2006;47:163—72.

[36] Streeter DD, Spotnitz HM, Patel D, Ross Jr J, Sonnenblick E.H. Fiber orientation in the canine left ventricle during diastole and systole. Circ Res 1969;24:339—47.

[37] Coghlan C, Hoffman J. Leonardo da Vinci's flights of the mind must continue: cardiac structure and the fundamental relation of form and function revisited. Eur J Cardiothorac Surg 2006;29:S4—7.

[38] Rushmer RF. Functional anatomy and control of the heart. In: Rushmer RF, editor. Cardiovascular dynamics. 4th ed. Philadelphia: WB Sounders Co; 1976. p. 76—131.

[39] Matsumoto T, Komori R. Functional anatomy of the heart. In: Matsuda K, editor. Japanese handbook of physiology, III physiology of circulation. Tokyo: Igaku Shoin Ltd; 1969. p. 70—110.

[40] Streeter Jr DD, Powere WE, Ross MA, Torrent-Gusp F. Three-dimensional fiber orientation in the mammalian left ventricular wall. In: Baan J, Noordergraaf A, Raines J, editors. Cardiovascular system dynamics, III ventricular dynamics. Cambridge: The MIT press; 1978. p. 73—84.

[41] Luisada AA. In: Luisada AA, editor. The sound of the normal heart. Saint Louis: Warren H Green Inc; 1972.

[42] Sakamoto T, Ichiyasu H, Hayashi T, Kawaratani H, Amano K, Hada Y. Genesis of the third heart sound, phono-cardiographic studies. Jpn Heart J 1976;17:150—62.

[43] Ueda H, Kaito G, Sakamoto T. Normal third heart sound. In: Ueda H, Kaito G, Sakamoto T, editors. Clinical phonocardiography. Tokyo: Med. Electro Times Co; 1978. p. 170—80.

[44] Rushmer RF. Cardiovascular dynamics. 4th ed Philadelphia: WB Sounders; 1976, p.425.